Journal of Inclusion Phenomena and Macrocyclic Chemistry **35:** 317–325, 1999.

Nematic Liquid Crystals as Media for Real-Time Holography

A. MINIEWICZ[1,⋆], S. BARTKIEWICZ[1], A. JANUSZKO[1] and J. PARKA[2]
[1]*Institute of Physical and Theoretical Chemistry, Wrocław University of Technology, 50-370 Wrocław, Poland;* [2]*Institute of Technical Physics, Military University of Technology, 00-908 Warsaw, Poland*

Abstract. We report on a novel type of orientational photorefractive devices consisting of dye-doped or pure nematic liquid crystals. These systems can be employed as the recording media for real-time (dynamic) holography. Optical addressing of liquid crystal molecules is facilitated due to the natural tendency of molecular self-assembling in nematics and their easy reorientation upon action of an electric field. This field can be produced by incoming light via photoconductivity either in the bulk or at the surface of the nematic liquid crystal layer. We present an experimental study of dynamic self-diffraction of light on thin phase holograms formed in a nematic liquid crystal panel. Optically addressed spatial light modulators designed by us can be the active elements of image processing systems and in this communication we demonstrate the optical correlator performing image recognition.

Key words: nematic liquid crystals, real-time holography, optically addressed spatial light modulators, image recognition

1. Introduction

Real-time holography is nowadays widely used in the area of optical image processing including pattern recognition, associative memory, optical filtering or moving object extraction. Materials that could be employed in this field must show capabilities of dynamic hologram recording/erasing in contrast to a conventional holographic material where the hologram is permanent. Ordered liquid crystalline (LC) materials especially nematics (NLC) can exhibit strong birefringence which can easily be modified by electric or magnetic fields [1]. This property has been widely used in many LC opto-electronic devices including optical switchers, retarders, LCTV screens and electrically addressed spatial light modulators (EA SLM's), the latter mostly used in input devices for supplying images or bit-pages into holographic optical systems. The growing interest in various photorefractive materials including crystals [2] and polymers [3] stimulated the research of photoactive LCs capable of reversible real-time recording of phase (i.e., refractive index) gratings via the mechanism of molecular reorientation by optically driven

⋆ Author for correspondence.

electric [4–8], mechanical [9] or surface forces [10, 11]. For dynamic holographic purposes it is necessary that the local light induced gratings may relax thereby preparing the medium for subsequent optical pattern recording. In many recent [12–15] papers it has been shown that the optical properties of homogeneously aligned NLC, particularly its birefringence $\Delta n = n_e - n_0$, can locally be changed by organized reorientation of the director $\hat{n}$ (a unit pseudovector pointing along the average direction of the long molecular axes of the NLC) over the disorienting influence of temperature ($\sim$kT). Among mechanisms leading to light induced refractive index changes in liquid crystals in transmission geometry of two-wave mixing experiment one should mention: nonlinear optical phenomena (electronic) [1]; optical Fréedericksz transition (reorientation) [16–18]; dye-enhanced optical Fréedericksz transition [19–22]; photocurrent induced director reorientations [4–6]; reorientation by photochemical photocyclization or trans-cis conformational rearrangements (fulgides, diaryl alkenes, spiropyrans and azobenzenes) [9, 23]; surface mediated LC alignment [10, 11]; temperature induced changes of an order parameter including induction of phase transition [24, 25] and chirooptical switching between LC phases [26].

In this paper we will focus on photocurrent induced director reorientation – the mechanism studied by us since 1995 [27] and proven to be effective both for processing of images as well as for other nonlinear optical processes like optical phase conjugation [28] or coherent light amplification [29]. In fact one can distinguish two mechanisms: one which occurs via a bulk charge carrier photogeneration in dye-doped NLC and the other occurring via space charge electric field produced by light within a photoconducting polymeric layer at the inner surface of an LC panel. The effectiveness of these processes (the magnitude of the amplitude of the induced refractive index grating Δn_K) depends on the specific design of LC panels as well as on physicochemical and optical parameters of used LCs. However, these two mechanisms are substantially different with respect to beam-coupling effects. The former allows for grating recording at any incidence angle but does not exhibit energy exchange between the beams in a two-wave mixing experiment. The second allows for grating recording only at oblique light incidence angles and like in a classic photorefractive effect exhibits an extremely high capability of beam-coupling effect: a transfer of energy from one beam to another.

The aim of this paper is to compare the two mentioned mechanisms with respect to their use for designing optically addressed spatial light modulators (OA SLMs) based on NLCs.

2. Experimental

For evaluation of a material's fundamental holographic properties (such as diffraction efficiency η and recording/erasing time constants) we used a two-wave mixing experiment (cf., Figure 1), in which two linearly s- or p-polarized coherent laser

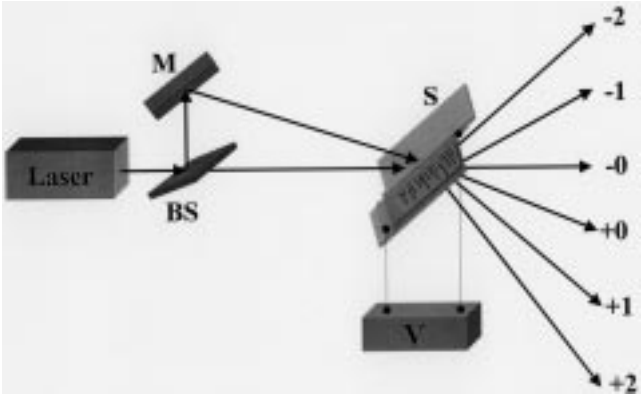

Figure 1. Schematic of the two wave-mixing experiment and self-diffraction of light on a thin grating formed in a LC panel. M, mirror, BS, beam splitter, S, liquid crystal panel, V, dc voltage supplier.

beams intersect within an optical medium and form a simple interference grating. We prepared two types of homogeneously aligned NLC panels (cf., Figure 2):

(i) a panel containing nematic liquid crystal doped by a dye showing the capability of photogeneration in the LC layer bulk the mobile charge carriers (ions);
(ii) a panel containing pure nematic liquid crystal but equipped with a transparent electrode made of photoconducting polymer.

In experiments showing the practical holographic properties of dye-doped liquid crystals (i) we used a nematic LC mixture ($\Delta\epsilon = +9.8$, $\Delta n = 0.1964$) doped with 0.4% of 1,4-dibutylamino-9,10-anthraquinone dye. The 10 μm thick cell was equipped with ITO conducting electrodes and covered with 100 nm thick polymide insulating and orienting layers (cf., Figure 2a). In the case of the pure liquid crystal equipped with a photoconducting polymeric layer (ii) we prepared a similar cell with a multicomponent nematic liquid crystal mixture E7 ($\Delta\epsilon = +13.8$, $\Delta n = 0.2253$) but its inner part, on one side, was covered with a 60 nm thick spin coated poly(3-octyl)thiophene photoconducting layer and on the other side with a 100 nm polymide layer (cf., Figure 2b). These polymeric layers were then uniaxially brushed in order to impose a planar ordering of the nematic liquid crystals filling the cells.

3. Results and Discussion

When a material is capable of changing its optical properties $\Delta n^{\text{eff}}(x)$ according to light intensity modulation produced by two plane waves $I(x) = I_0(1+m\cos(Kx))$ a self-diffraction of laser beams occurs resulting in an appearance of multiple

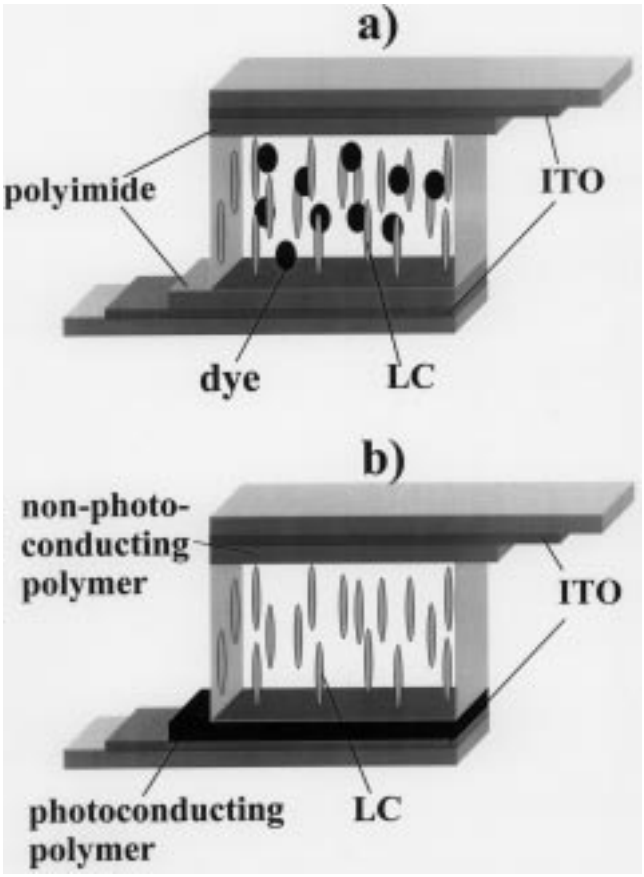

Figure 2. Dye-doped liquid crystal cell (a) and a pure liquid crystal cell with a photoconducting polymeric layer (b).

order diffraction spots (0, ± 1, ± 2, ..., cf., Figure 1). The period Λ of the grating ($K = 2\pi/\Lambda$ is the grating wavevector) depends on the angle θ between the crossed light beams in a two-wave mixing experiment ($\Lambda = \lambda/2n \sin(\theta/2)$, where λ is the laser light wavelength and n is the average index of refraction of the medium). The measurement of the self-diffraction characteristics like the diffraction efficiency (a ratio of diffracted and incident light intensities $\eta = I_{\text{diffracted}}/I_{\text{incident}}$), the time constants of grating formation and decay (τ_r and τ_d), the resolution (number of lines recorded per millimetre) and the exponential gain factor (Γ a factor measuring beam-coupling efficiency and optical gain) deliver information necessary for evaluation of important material parameters. In the first approximation the light diffraction efficiency η is dependent on the amplitude of the light induced birefringence Δn^{eff} in the grating and the grating thickness (in this case the thickness of the liquid crystal layer L). As we deal with a Raman–Nath diffraction regime a first order diffraction efficiency: $\eta = |J_1(\phi)|^2$ where J_1 is the 1st order Bessel

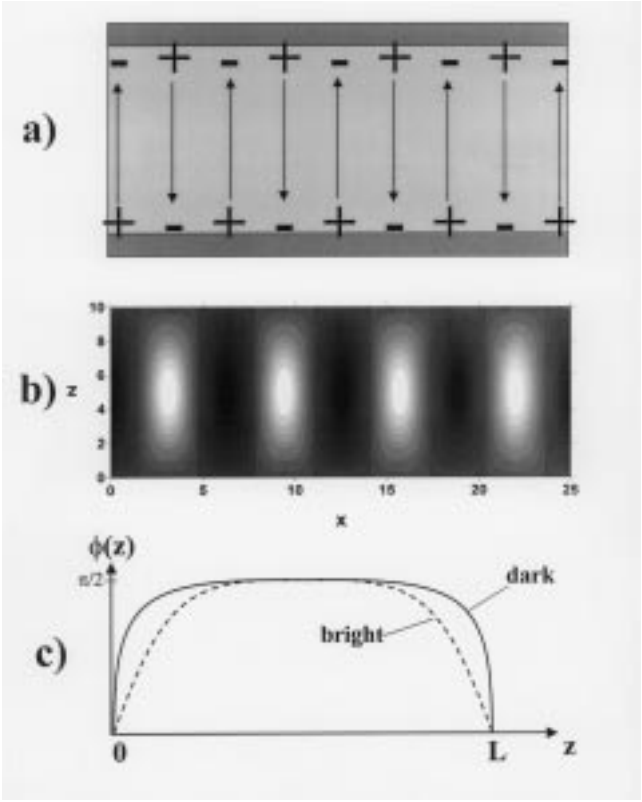

Figure 3. Schematic view of the incremental electric field lines induced by sinusoidal light in a dye-doped liquid crystal cell (a), the index of refraction changes (b) and profiles of director reorientation (c) in the dark and bright regions of the interference fringe.

function and $\phi = 2\pi \Delta n^{\text{eff}} L \lambda^{-1}$. Generally η is a strong function of a dc biasing field applied to the liquid crystal layer [6, 8, 27]. This field pretilts the initially homogeneously aligned molecules $\varphi = 0$ inducing a field dependent distribution of molecular reorientation angles $\varphi(E_z(x, y, z))$ along the layer thickness L toward a near homeotropic alignment for which $\varphi = \pi/2$. This has an influence on the average index of refraction of the NLC layer seen by extraordinary polarized light [1]:

$$n_e^{\text{eff}}(x, y, z) = \frac{1}{L} \int_L \mathrm{d}z \times \frac{n_e n_0}{\sqrt{n_0^2 \sin^2[\varphi(E_z(x, y, z))] + n_e^2 \cos^2[\varphi(E_z(x, y, z))]}} \quad (1)$$

where $E_z(x, y, z)$ is a z component of the local electric field interacting with molecular dipoles, n_e and n_0 are the extraordinary and ordinary refractive indices. In a

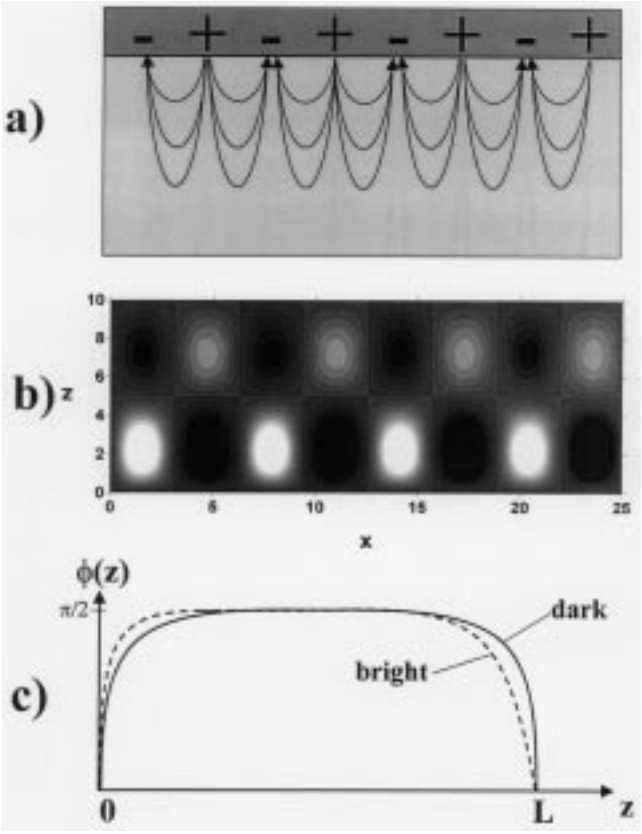

Figure 4. Schematic view of the incremental electric field lines induced by sinusoidal light in a liquid crystal cell with a photoconducting polymeric layer at the top (a), the index of refraction changes (b) and profiles of director reorientation (c) in the dark and bright regions of the interference fringe. Note the light induced asymmetry of the LC director profile.

typical hologram recording procedure the incoming light having sinusoidal intensity pattern is slightly absorbed by the dye and creates mobile charge carriers either in the bulk of the NLC layer (case i) or in the polymeric electrode when absorbed within the polymer (case ii). The subsequent redistribution of the photogenerated charge carriers either mostly by drift along the z-axis within the bulk of the LC (case i, Figure 3a) or mostly by diffusion along the x-axis within a polymeric layer (case ii, Figure 4a) results in a spatial modification of electric field acting on NLC molecules. However, this modification is substantially different for both described cases due to the different dominant mechanisms of charge redistribution processes. The dominating light induced increments to externally applied field are shown schematically for both described cases as the lines of electric field. This leads to the creation of complex refractive index gratings shown schematically in Figure 3b and Figure 4b where the brighter regions are assigned to a lower refractive index and darker to its higher values. The shapes of the angular distribution function $\varphi(E_z(x,$

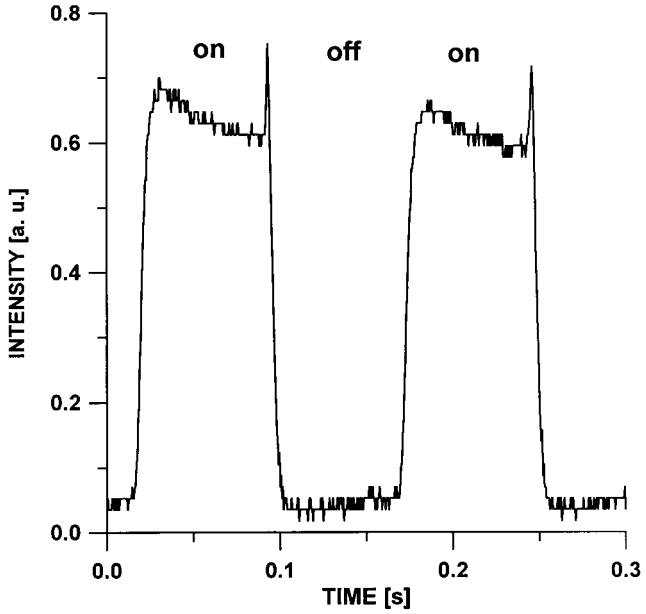

Figure 5. Kinetics of grating recording and erasure in a two-wave mixing experiment performed with the liquid crystal panel equipped with a photoconducting polymeric layer biased by 20 V. The oscilloscope trace shows the intensity of the first order diffracted light when one of the beams is interrupted (an off state).

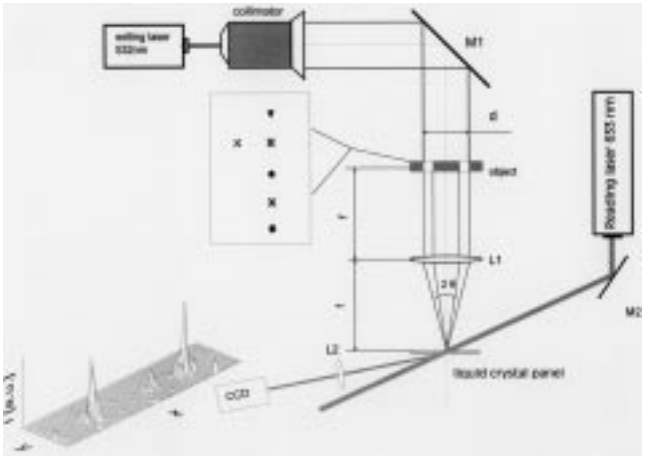

Figure 6. Schematic view of a simple joint-Fourier-transform optical correlator performing image recognition of a cross (the object plane) and the resulting two correlation peaks seen by a CCD camera at the correlation plane. These two peaks correspond to two crosses seen in the column.

y, z)) of the director of NLC illuminated by light and dark regions for the two described cases are given in Figure 3c and Figure 4c. The full analytical description of this function is not known yet and will be the subject of further theoretical and experimental studies. From the theory of light diffraction on periodic gratings one can deduce that energy transfer between the beams is possible only for the grating shown in Figure 4 at oblique light incidence, because in that case the necessary shift between the refractive index grating and the light interference pattern is equal to $\pi/2$ [29].

The kinetics of grating recording and its erasure in the presence of a single beam is a function of the liquid crystal parameters among which the viscosity, the dielectric constants, the anchoring forces and the elastic constants play crucial roles. The response times depend as well on external parameters like a voltage applied to the cell, an intensity of recording light and a grating spacing. The example of response time for E7 NLC mixture in the cell equipped with photoconducting polymer is shown in Figure 5. One can notice that within a $\approx$30 m s time period a hologram (simple sinusoidal grating) can be written and erased. The diffraction efficiencies η observed in the same system vary between 1 to 20% depending on the experimental conditions. Self-diffraction is observed for incoming light intensities I_0 as weak as 50 μW/cm^2 though most of the experiments described in this communication were done at light intensities of 300 mW/cm^2. The biasing voltages employed by us were in the range 1–30 V depending on the characteristics of the LC panels.

The liquid crystal cells described here were tested for their reliability in systems for optical processing of information in which conditions of light illumination are considerably different from those used in two-wave mixing experiments. In Figure 6 we schematically show an example of a simple joint-Fourier-transform (JFT) optical correlator assembled by us. The detailed description of this correlator and its characteristics can be found in Ref. [30]. The heart of the system is the photosensitive liquid crystalline optically addressed spatial light modulator (OA SLM) able to record holograms and be ready for the next use in as short a time as 30 m s. In the inset to Figure 6 we show the experimental results for optical correlation between two input images: the cross and the column of different symbols, superimposed on the laser beam with the help of a computer-driven EA SLM. The optical correlator is able to identity the two crosses and their position within the column in a real-time procedure. Two marked correlation peaks seen by a CCD camera correspond to recognized images (in Figure 6 they are shown in a 3-D plot). The resolution of the system is sufficient to recognize much more complicated images [30].

Acknowledgements

This work has been performed on equipment obtained from the Foundation for Polish Science. The collaboration with Dr F. Kajzar (CEA, Saclay) within the POLONIUM programme is gratefully acknowledged.

References

1. I. C. Khoo: *Liquid Crystals Physical Properties and Nonlinear Optical Phenomena*, J. Wiley, New York (1995).
2. P. Günter and J.-P. Huignard (eds.): *Photorefractive Materials and their Applications*, Vols. 1 and 2, Springer Verlag, Berlin (1988).
3. K. Meerholz, B. L. Volodin, Sandalphon, B. Kippelen, and N. Peyghambarian: *Nature* **371**, 497 (1994).
4. I. C. Khoo: *Optics Lett.* **20**, 2137 (1995).
5. E. V. Rudenko and A. V. Sukhov: *JETP (in Russian)* **105**, 1621 (1994).
6. S. Bartkiewicz, A. Miniewicz, A. Januszko, and J. Parka: *Pure Appl. Optics* **5**, 799 (1996).
7. I.-C. Khoo: *IEEE J. Quant. Electron*. **32**, 525 (1996).
8. A. Miniewicz, S. Bartkiewicz, W. Turalski, and A. Januszko: *Dye-Doped Liquid Crystals for Real-Time Holography*, in R. W. Munn, A. Miniewicz, and B. Kuchta (eds.), *Electrical and Related Properties of Organic Solids*, NATO ASI Series, **3/24**, Kluwer Academic Publishers, Dordrecht, pp. 323–337 (1997).
9. B. Saad, T. V. Galstyan, M. M. Denariez-Roberge, and M. Dumont: *Opt. Commun.* **151**, 235 (1998).
10. W. M. Gibbons, P. J. Shannon, S.-T. Sun, and B. J. Swetlin: *Nature* **351**, 49 (1991).
11. H. Knobloch, H. Orendi, B. Stiller, M. Büchel, W. Knoll, T. Seki, S. Ito, and L. Brehmer: *Syn. Met.* **81**, 297 (1996).
12. A. G. Chen and D. J. Brady: *Opt. Letters* **17**, 441 (1992).
13. T. Ikeda, O. Tsutsumi, and T. Sasaki: *Syn. Met.* **81**, 289 (1996).
14. H. Ono and N. Kawatsuki: *Appl. Phys. Lett.* **71**, 1162 (1997).
15. G. P. Wiederrecht, B. A. Yoon, and M. R. Wasielewski: *Science* **270**, 1794 (1995).
16. H. Li, Y. Liang, and I. C. Khoo: *Mol. Cryst. Liq. Cryst*. **251**, 85 (1994).
17. A. Sugimura and O.-Y. Zhong-can: *Phys. Rev*. **A 45**, 2439 (1992).
18. I. C. Khoo, H. Li, and Y. Liang: *IEEE J. Quant. Electron.* **29**, 1444 (1993).
19. I. Jánossy: *Phys. Rev. E* **49**, 2957 (1994).
20. I. Jánossy, A. D. Lloyd, and B. S. Wherrett: *Mol. Cryst. Liq. Cryst.* **179**, 1 (1990).
21. I. Jánossy, L. Csillag, and A. D. Lloyd: *Phys. Rev*. **A 44**, 8410 (1991).
22. I. Jánossy and T. Kôsa: *Optics Lett*. **17**, 1183 (1992).
23. B. L. Feringa, W. F. Jager, and B. de Lange: *Tetrahedron* **49**, 8267 (1993).
24. I.-C. Khoo, P. Y. Yan, G. M. Finn, T. H. Liu, and R. R. Michael: *J. Opt. Soc. Am.* **B85**, 202 (1988).
25. P. Y. Yan and I.-C. Khoo: *IEEE J. Quant. Electron.* **25**, 520 (1989).
26. B. L. Feringa, N. P. M. Huck, and A. M. Schoevaars: *Adv. Mater.* **8**, 681 (1996).
27. S. Bartkiewicz and A. Miniewicz: *Adv. Mat. Opt. Electron.* **6**, 219 (1996).
28. A. Miniewicz, S. Bartkiewicz, and J. Parka: *Optics Commun.* **149**, 89 (1998).
29. A. Miniewicz, S. Bartkiewicz, and F. Kajzar: *Nonlinear Optics* **19**, 157 (1998).
30. S. Bartkiewicz, P. Sikorski, and A. Miniewicz: *Optics Lett.* **23**, 1769 (1998).